IEEE Access
Multidisciplinary | Rapid Review | Open Access Journal

Date of publication xxxx 00, 0000, date of current version xxxx 00, 0000.

Digital Object Identifier 10.1109/ACCESS.2017.DOI

Resource Allocation for CoMP in Cellular Networks with Base Station Sleeping

YOGHITHA RAMAMOORTHI, (Student Member, IEEE) AND ABHINAV KUMAR, (Member, IEEE)
Department of Electrical Engineering, Indian Institute of Technology Hyderabad, Telangana, 502285 India (e-mail: {ee15resch02007,abhinavkumar}@iith.ac.in)
Corresponding author: A. Kumar (abhinavkumar@iith.ac.in).

ABSTRACT Base station sleeping (BSS) can result in significant reduction in energy consumption of cellular networks during low traffic conditions. We show that the coverage loss due to BSS can be compensated via coordinated multi-point (CoMP) based transmission in a cluster of base stations. For a BSS with CoMP based system, we propose various BSS patterns to achieve suitable trade-offs between energy savings and throughput. We formulate the CoMP resource allocation and $\alpha-$Fair user scheduling as a joint optimization problem. We derive the optimal time fraction and user scheduling for this problem and use it to formulate a simplified BSS with CoMP optimization problem. A heuristic that solves this problem is presented. Through extensive simulations, we show that suitable trade-offs among energy, coverage, and rate can be achieved by appropriately selecting the BSS pattern, CoMP cluster, and rate threshold.

INDEX TERMS α-Fair throughput, base station sleeping (BSS), cellular networks, coordinated multi-point (CoMP) transmission, downlink, energy.

I. INTRODUCTION

The significant increase in demand of data has led to the deployment of a huge number of base stations (BSs) in cellular networks. The BSs consume nearly 80% of the total energy consumed in cellular networks [1], out of which 70% is consumed by power amplifiers, processing circuits, and air conditioners [2]. These BSs are typically designed and deployed for peak user demands. However, it has been shown in [3] that the user demand varies with time resulting in underutilized BSs and switching off some BSs during low user demand results in significant energy savings. Further, in [4], it has been shown that around 2% of global Carbon emission is from cellular networks. Thus, base station sleeping (BSS) during low user demand is advantageous for both economical and ecological reasons, i.e., reduction in energy consumption and Carbon footprint of the network, respectively.

In [3], a dynamic BSS strategy has been studied based on the spatial and temporal traces of real-time downlink traffic. It has been shown in [5] that upto 30% energy can be saved in a cellular network through BSS. In [6], the energy and throughput trade-off for a given coverage has been evaluated. To overcome the coverage constraint in BSS, infrastructure sharing through multi-operator service level agreements has been proposed in [7]. A small cell based approach for BSS has been presented in [8] and [9]. Further, a dynamic BSS strategy based on hybrid energy supplies has been presented in [10].

A promising approach for increasing edge users performance (equivalently coverage) in cellular networks is coordinated multi-point (CoMP) based transmission and reception. Joint transmission (JT) and coordinated scheduling/beamforming are the two variants of CoMP that have been discussed in [11]. In this work, we consider only CoMP with JT for our analysis and use CoMP with JT interchangeably with CoMP throughout the text. A coverage probability based analysis of CoMP systems using stochastic geometry has been derived in [12]. Further, in [13], it has been shown through analysis that CoMP can improve coverage upto 17%. The resource allocation for CoMP has been presented in [14]. A new scheduling policy for two tier CoMP network with one macro-cell and multiple small cells has been proposed in [15]. However, BSS with CoMP has been studied recently.

Two key requirements from the perspective of the upcoming 5G cellular networks are higher spectral efficiency and energy efficiency [16]. BSS with CoMP can possibly offer both. In this direction, a stochastic geometry based analysis of outage and coverage probabilities for BSS with CoMP has been performed in [17]. In [18], the outage probability for a hexagonal grid model of BSS with CoMP in terms of signal-to-noise-ratio (SNR) has been derived. The energy efficiency analysis of BSS with CoMP, under the constraint that only one BS can be switched off in a cluster, has been obtained in [19]. The fundamental trade-off between energy efficiency and spectral efficiency for BSS with CoMP taking backhaul

This article has been accepted for publication in a future issue of this journal, but has not been fully edited. Content may change prior to final publication. Citation information: DOI 10.1109/ACCESS.2017.2783398, IEEE Access

power consumption into account has been discussed in [20]. The performance of BSS with CoMP taking only uplink into consideration has been recently investigated in [21]. Enlarged coverage and improved energy savings for BSS with CoMP has been presented in [22]. However, the trade-off with respect to users' throughput has not been considered in [22]. A recent study on JT variant of CoMP has been presented in [23] that shows improvements in throughput at the cost of outage probability. The trade-off between energy, coverage, and throughput for BSS with CoMP has not been jointly studied in the literature. Further, suitable resource allocation schemes for BSS with CoMP that achieve these trade-offs are required. This is the motivation of this work.

From the perspective of resource allocation in CoMP, the time fractions allocated to CoMP and non-CoMP users have been assumed in [15]. Further, for these assumed time fractions, the user rates have been computed for a round robin scheduler. Numerical methods for solving the CoMP resource allocation problem have been discussed in [20] and [22]. In our own prior work [21], the uplink based resource allocation has been performed with assumed CoMP time fraction. However, no closed form results have been derived. Hence, we additionally derive the optimal CoMP and non-CoMP time fractions for a more generic $\alpha-$Fair scheduler in this work. To the best of our knowledge, this is the first work that considers various possible CoMP configurations, derives optimal time fraction of CoMP, an optimal scheduler, and use them in the context of BSS for improved energy and spectral efficiency in cellular networks.

The contributions of this paper are as follows.

- Various possible CoMP configurations and BSS patterns are proposed and compared.
- The joint BSS and CoMP optimization problem is shown to be a mixed integer non-linear program (MINLP). This is further decomposed into CoMP and BSS with CoMP optimization problems.
- The decomposed problem of joint resource allocation and user scheduling for CoMP is solved using method of Lagrange multipliers through the Karush Kuhn Tucker (KKT) approach [24].
- This is the first work that derives the optimal user scheduling for CoMP and non-CoMP users, and the optimal resource allocation for a CoMP cluster for an $\alpha-$Fair scheduler. Note that the derived CoMP results in this work are independent of the BSs' topology. Thus, the results are also valid for random BSs' locations.
- The optimal CoMP solutions are used to re-frame a BSS with CoMP optimization problem that is relatively less complex.
- A dynamic heuristic is proposed that solves the optimization problem for an energy efficient point of operation without compromising on coverage or user rates.

The organization of the paper is as follows. The system model is described in Section II. The Joint BSS and CoMP problem is formulated and analysed in Section III. In Section IV, resource allocation and user scheduling for the decomposed CoMP problem is presented as an optimization problem along with the derivation of the optimal solutions. The simplified BSS with CoMP optimization problem is re-framed in Section V. A novel heuristic that solves the BSS with CoMP problem is described in Section VI. Extensive numerical results are presented in Section VII. Some concluding remarks along with possible future works are discussed in Section VIII.

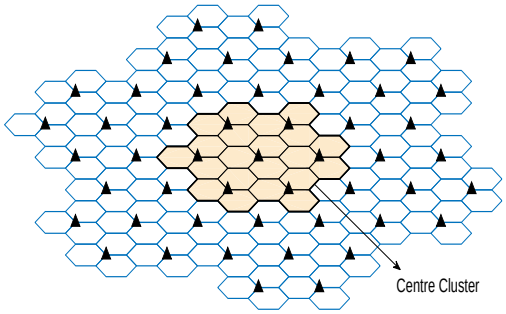

FIGURE 1: Benchmark system with the wraparound layout around center cluster (reuse factor 1).

II. SYSTEM MODEL

A. BENCHMARK SYSTEM

We consider a homogeneous OFDMA based LTE cellular network as shown in Fig. 1. The set of BSs and corresponding sectors in the network are denoted by $\mathcal{B} = \{1, 2, ..., B\}$ and $\mathcal{S} = \{1, 2, ..., S\}$, respectively. Note that the BSs are represented by triangles in Fig. 1. The hexagons represent the corresponding sectors of a BS such that each BS has three sectors. Without any loss of generality, we assume that the set of sectors is ordered with the set of BSs. Hence, any BS $b \in \mathcal{B}$ corresponds to the sectors $3b-2$, $3b-1$, and $3b$, in the set $\mathcal{S}$. For example, in Fig. 2a, BS 4 corresponds to sectors 10, 11, and 12. We denote the set of users in the system by $\mathcal{U} = \{1, 2, ..., U\}$. We consider that the users are uniformly distributed in the system for a given user density μ. Let $\mathcal{M} = \{1, 2, ..., M\}$ denote the set of subchannels available in the network. We consider a reuse factor of 1. Hence, a total of M subchannels are allocated to each sector in $\mathcal{S}$. A comprehensive list of mathematical notations used in this paper is presented in Table 1. Next, we present the channel model considered in this paper.

B. CHANNEL MODEL

We consider a time division duplex (TDD) system. For mathematical brevity, we assume a frequency flat channel model and focus on the downlink. However, a similar analysis is possible for a frequency selective channel and uplink. The

This article has been accepted for publication in a future issue of this journal, but has not been fully edited. Content may change prior to final publication. Citation information: DOI 10.1109/ACCESS.2017.2783398, IEEE Access

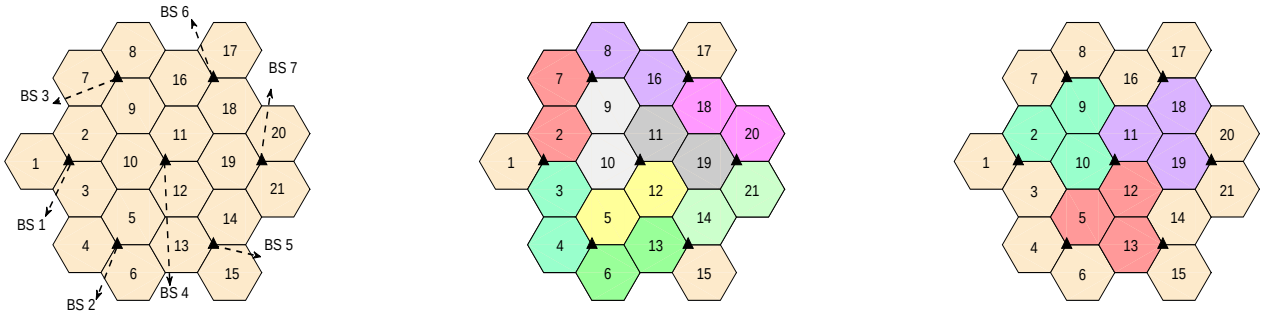

(a) Configuration 1 (C_1) (b) Configuration 2 (C_2) (c) Configuration 3 (C_3)

FIGURE 2: Various CoMP configurations for the center cluster.

TABLE 1: Mathematical notations.

C_i	CoMP configurations
G_s	Antenna directivity gain
$h^m_{u,s}$	Channel gain at user u from sector s on the subchannel m
P^m_s	Power allocated per subchannel m by sector s
$r_{u,s}$	Link rate of user u from sector s
$x_{u,s}$	Binary association variable of user u with sector s
w_b	Binary BSS variable of BS b
$z_{u,s}$	Binary CoMP variable of user u in sector s
α	Fairness parameter for the α-Fair scheduler
$\beta_{u,s}$	Time fraction allocated for user u by a sector s
$\beta_{u,k}$	Time fraction allocated for user u by a virtual cluster k
$\eta(.)$	Spectral efficiency in $bits/symbol$
Γ_d	CoMP SINR threshold in dB
$\gamma^m_{u,s}$	Received SINR of user u from a sector s
$\gamma^m_{u,k}$	Received SINR of user u from a virtual cluster k
θ_k	Optimal CoMP time fraction of a virtual cluster k
λ_u	Downlink rate for a user u
μ	User density per km^2
$\mathcal{B}$	Set of BSs with order B
$\mathcal{B}_q$	Set of BSs in the cluster q
$\mathcal{E}$	Percentage energy saved
$\mathcal{K}_q$	Set of virtual clusters in cluster q
$\mathcal{M}$	Set of subchannels with order M
$\mathcal{Q}$	Set of clusters with order Q
R	Rate threshold
$\mathcal{S}$	Set of sectors with order S
$\mathcal{S}_k$	Set of sectors in virtual cluster k
$\mathcal{T}_\alpha$	α-Fair throughput
$\mathcal{U}$	Set of users
$\mathcal{U}_k$	Set of users in virtual cluster k
$\mathcal{V}_q$	Set of users in the cluster q
$\mathcal{W}_q$	Set of sectors in cluster q
$\mathcal{Z}_{a1/a2}$	BSS pattern where $a1$ out of $a2$ BSs are switched off
$\mathbb{U}$	Utility function for α-Fair scheduler
$\lvert.\rvert$	Cardinality of a set
$\lceil.\rceil$	Ceil the input to smallest following integer

downlink signal-to-interference-plus-noise ratio (SINR) of a user u from a sector s, denoted by $\gamma^m_{u,s}$, on a subchannel m is given as

$$\gamma^m_{u,s} = \frac{P^m_s h^m_{u,s}}{\sum\limits_{\substack{\hat{s}\neq s \\ \hat{s}\in\mathcal{S}}} P^m_{\hat{s}} h^m_{u,\hat{s}} + \sigma^2}, \tag{1}$$

where, P^m_s is the power allocated to the subchannel m by the sector s, $\sum\limits_{\substack{\hat{s}\neq s \\ \hat{s}\in\mathcal{S}}}^{m} P^m_s h^m_{u,\hat{s}}$ is the interference on the subchannel m, σ^2 is the noise power, and $h^m_{u,s}$ denotes the channel gain between the sector s and the user u. The channel gain is given by

$$h^m_{u,s} = 10^{\left(\frac{-PL(d)+G_s(\phi)+G_u-\upsilon-\rho}{10}\right)}, \tag{2}$$

where, G_u is the antenna gain, υ is the penetration loss, ρ is the loss due to fading and shadowing, $PL(d)$ is the path loss for the distance d between u and s, and $G_s(\phi)$ is the directivity gain equal to

$$G_s(\phi) = 25 - min\left\{12\left(\frac{\phi}{70}\right)^2, 20\right\}, \forall -\pi \leq \phi \leq \pi, \tag{3}$$

in which ϕ denotes the angle between the u and the main lobe orientation of s [25].

C. RESOURCE ALLOCATION AND USER SCHEDULING

Let P_{BS} denote the total transmit power of a BS. Then, given that the BS transmit power is shared among the three sectors of a BS, the power allocated in a sector s per subchannel m, P^m_s, is given by

$$P^m_s = \frac{P_{BS}}{3M}, \quad \forall\, s \in \mathcal{S},\ m \in \mathcal{M}. \tag{4}$$

There exist energy efficient power allocation schemes in the literature [26] which save energy through efficient transmit power allocation. However, it has been shown in [26] that the energy savings through BSS is an order of magnitude higher than energy efficient power allocation schemes. Thus, in this work, we consider uniform power allocation such that the available transmit power per BS is allocated equally among all available subchannels across all the sectors in a BS. This also corresponds to frequency flat fading. The presented analysis can be generalized to frequency selective fading by using water filling based power allocation schemes as discussed in [27].

This article has been accepted for publication in a future issue of this journal, but has not been fully edited. Content may change prior to final publication. Citation information: DOI 10.1109/ACCESS.2017.2783398, IEEE Access

TABLE 2: Modulation and coding scheme [28].

SINR Threshold (dB)	-6.5	-4	-2.6	-1	1	3	6.6	10	11.4	11.8	13	13.8	15.6	16.8	17.6
Efficiency (bits/symbol)	0.15	0.23	0.38	0.60	0.88	1.18	1.48	1.91	2.41	2.73	3.32	3.9	4.52	5.12	5.55

We use $\eta(\gamma_{u,s}^m)$ to denote the spectral efficiency achieved by a user in bits/symbol. The value of $\eta(\gamma_{u,s}^m)$ obtained from an adaptive modulation and coding scheme (MCS) is given in Table 2 for various ranges of SINR [28]. Given $\gamma_{u,s}^m$ as in (1), the link rate for the user u from sector s, denoted by $r_{u,s}$, is expressed as

$$r_{u,s} = \frac{\eta(\gamma_{u,s}^m)\, SC_{OFDM}\, SY_{OFDM}}{T_{sc}} M\,, \tag{5}$$

where, SC_{OFDM}, SY_{OFDM}, and T_{sc} represent the number of subcarriers per subchannel, number of symbols used per subcarrier, and time duration of a subframe, respectively. The factor M represents number of subchannels used in downlink per sector s.

We consider an $\alpha-$Fair time based scheduler at each sector s such that the scheduler allocates all the M subchannels for a downlink time fraction denoted by $\beta_{u,s}$ to a user u associated with it. In the benchmark system, we assume that any user u associates with the sector s from which it receives maximum received SINR on the downlink. Thus, for a user u, $\beta_{u,s}$ is non-zero for only one sector s. The resultant downlink rate for any user u, represented by λ_u, is given by

$$\lambda_u = \sum_{s\in\mathcal{S}} \beta_{u,s} r_{u,s}\,, \tag{6}$$

where, $r_{u,s}$ is the link rate as computed in (5). The utility function for an α-Fair user scheduler is expressed as [29]

$$\mathbb{U}_\alpha(\lambda) = \begin{cases} \dfrac{\lambda^{1-\alpha}}{1-\alpha}, & \alpha > 0,\ \alpha \neq 1, \\ log(\lambda), & \alpha = 1. \end{cases} \tag{7}$$

To focus on the downlink, we consider the TDD downlink time fraction as one, i.e., the fraction of time allocated for downlink is unity.

D. COMP

We consider that the sectors are grouped in pre-determined CoMP clusters such that only sectors from the same CoMP cluster can cooperate and perform CoMP. This is a reasonable assumption as CoMP requires a direct backhaul link between participating sectors. We denote the set of CoMP clusters by $\mathcal{Q} = \{1, 2, ..., Q\}$. Without loss of generality, we focus on the center cluster in Fig. 1 represented by q such that $\mathcal{B}_q$, $\mathcal{W}_q$, and $\mathcal{V}_q$ denote the set of BSs, sectors, and users in the cluster q, respectively. Within the cluster q, several configurations are possible for CoMP based on which sectors perform CoMP together. We represent set of CoMP sectors present in a cluster q as virtual clusters, which is represented by $\mathcal{K}_q = \{1, 2, ..., K\}$. In a virtual cluster k, we use $\mathcal{S}_k$ and $\mathcal{U}_k$ to represent the set of sectors and users, respectively. Thus, a cluster is a group of BSs that performs CoMP, and virtual cluster is the group of sectors within a cluster which performs CoMP. Thus, $\mathcal{S}_k \subseteq \mathcal{W}_q \subset \mathcal{S}$. We consider the following three possible CoMP configurations in the cluster q.

- Configuration 1: In this configuration, also referred to as C_1, as shown in Fig. 2a, a CoMP user in cluster q receive signals jointly from all sectors of BSs in the cluster q. Thus, the virtual cluster is of size $|\mathcal{W}_q|$ for C_1
- Configuration 2: In C_2, at most two sectors coordinate with each other as shown in Fig. 2b. Thus, sectors 1, 15, and 17 do not perform CoMP, while all the other sectors perform CoMP pairwise (sectors with the same colors cooperate).
- Configuration 3: In Fig. 2c, the Configuration 3 or C_3 is presented. The sectors in sets of three namely, {2, 9, 10}, {5, 12, 13}, and {11 , 18, 19} perform CoMP and the other sectors in the cluster q operate without CoMP in C_3.

To focus on other aspects like user scheduling and resource allocation for energy saving we have considered a cluster of 7 BSs and only three CoMP configurations. However, both the cluster size and the CoMP configurations can be adapted for a practical system. The sectors present in any virtual cluster $\mathcal{S}_k$ will vary based on the configuration under consideration as shown in Fig. 2.

We consider that the CoMP based system allocates a fraction of time for CoMP users in which the sectors in the virtual cluster transmit jointly on the downlink to the CoMP users. Whenever the SINR of a user u associated to a sector s, in the virtual cluster k, is less than a predetermined SINR threshold Γ_d, the user is served as a CoMP user. Let θ_k denote the time fraction in which such CoMP users receive data jointly from their virtual cluster k. During the remaining downlink time fraction $(1-\theta_k)$, each sector transmits to the typical non-CoMP users individually. Note that each virtual cluster k has its own θ_k.

In the CoMP time fraction θ_k, the downlink SINR received by a user u from any virtual cluster k of over subchannel m (denoted by $\gamma_{u,k}^m$) is given by

$$\gamma_{u,k}^m = \frac{\sum\limits_{v\in\mathcal{S}_k} P_v^m h_{u,v}^m}{\sum\limits_{\substack{\hat{v}\in\mathcal{S} \\ \hat{v}\notin\mathcal{S}_k}} P_{\hat{v}}^m h_{u,\hat{v}}^m + \sigma^2}\,, \tag{8}$$

where, $\sum\limits_{v\in\mathcal{S}_k} P_v^m h_{u,v}^m$ is the sum of the received powers for user u from all the sectors in the virtual cluster k and $\sum\limits_{\substack{\hat{v}\in\mathcal{S} \\ \hat{v}\notin\mathcal{S}_k}} P_{\hat{v}}^m h_{u,\hat{v}}^m$ is the interference from all the other sectors in the system which are not part of this virtual cluster k. Note that the SINR for users associated with the non-CoMP sectors and non-CoMP users of CoMP sectors of cluster q will be as in (1). The link

This article has been accepted for publication in a future issue of this journal, but has not been fully edited. Content may change prior to final publication. Citation information: DOI 10.1109/ACCESS.2017.2783398, IEEE Access

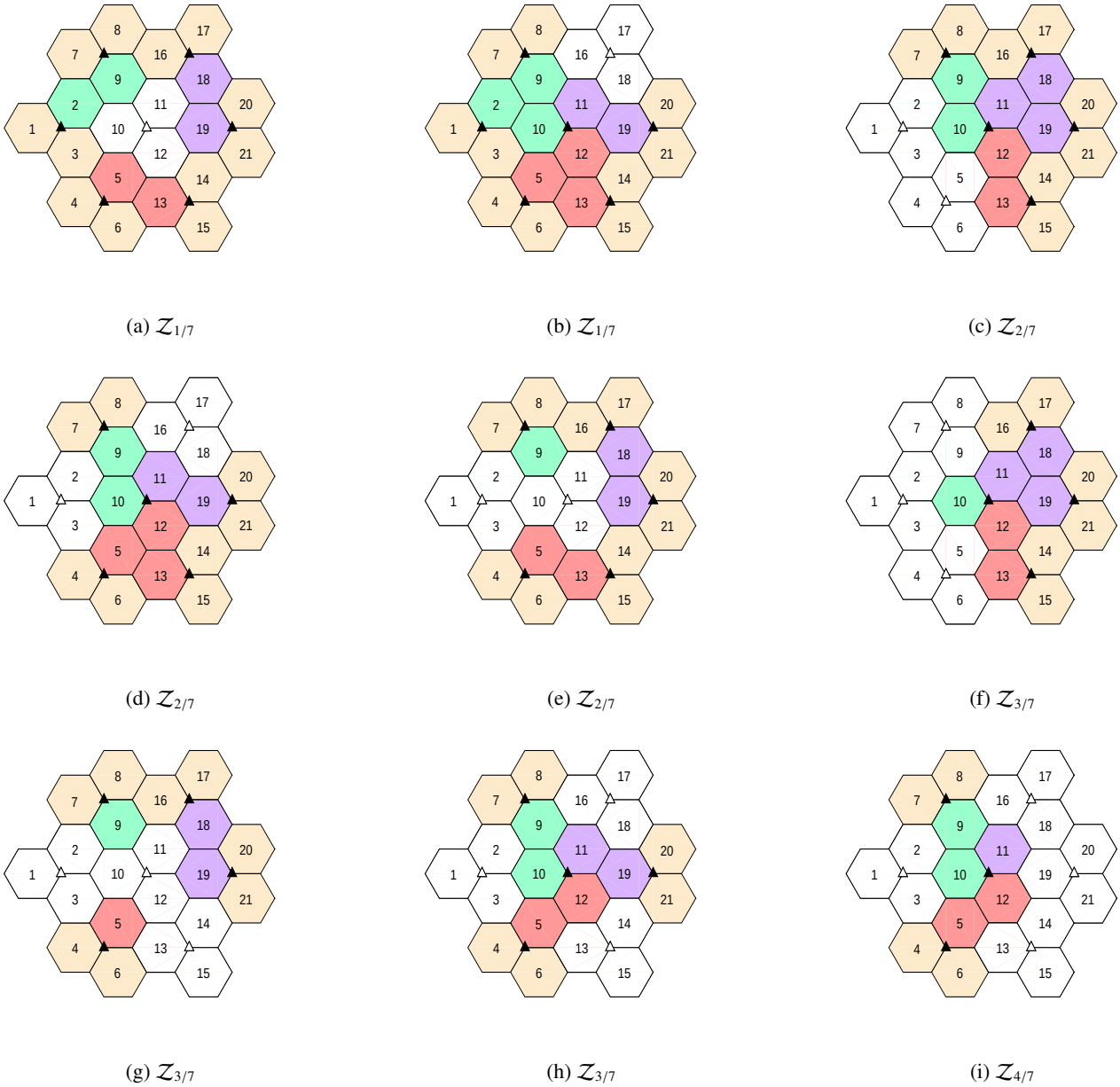

(a) $\mathcal{Z}_{1/7}$ (b) $\mathcal{Z}_{1/7}$ (c) $\mathcal{Z}_{2/7}$

(d) $\mathcal{Z}_{2/7}$ (e) $\mathcal{Z}_{2/7}$ (f) $\mathcal{Z}_{3/7}$

(g) $\mathcal{Z}_{3/7}$ (h) $\mathcal{Z}_{3/7}$ (i) $\mathcal{Z}_{4/7}$

FIGURE 3: Various BSS patterns for the center cluster for CoMP configuration 3 (the solid black triangles represent BSs in ON state and white triangles represents BSs that are in OFF state).

rate for a CoMP user u from a virtual cluster k can be obtained using (5) and (8) as

$$r_{u,k} = \frac{\eta(\gamma^m_{u,k})\, SC_{OFDM}\, SY_{OFDM}}{T_{sc}} M\,. \tag{9}$$

Next, we present the various BSS patterns considered in this work.

E. BSS PATTERNS

Let $\mathcal{Z}_{a1/a2}$ denote a BSS pattern in which a1 out of the total a2 BSs in the cluster are switched off. Hence, if a1 is equal to 0, then all BSs in the cluster are active. In Fig. 3, we depict some of the possible BSS patterns corresponding to $\mathcal{Z}_{1/7}$, $\mathcal{Z}_{2/7}$, $\mathcal{Z}_{3/7}$, and $\mathcal{Z}_{4/7}$ for CoMP configuration C_3. The shaded black triangles represent active BSs and white triangles represent the BSs that have been switched off in Fig. 3. We use idle and active states of the BSs with OFF and ON state interchangeably throughout the text. Note that Fig. 2c represents $\mathcal{Z}_0$ for C_3, where all BSs are active. For a given $a1$ in $\mathcal{Z}_{a1/a2}$, multiple possible BSS patterns exist. For example, Fig. 3a and Fig. 3b are both for $\mathcal{Z}_{1/7}$. Seven such combinations are possible for $\mathcal{Z}_{1/7}$ in which any one of the seven BS in the cluster can be switched off. The proposed optimization problem and the solution heuristic are valid for

This article has been accepted for publication in a future issue of this journal, but has not been fully edited. Content may change prior to final publication. Citation information: DOI 10.1109/ACCESS.2017.2783398, IEEE Access

all such combinations.

F. PERFORMANCE METRICS

The three key system performance metrics of a cellular network are rate, coverage, and energy. We measure the system performance of user rates through the $\alpha-$Fair throughput obtained over a cluster q as follows [29]

$$\mathcal{T}_\alpha = \begin{cases} \left(\frac{1}{|\mathcal{V}_q|} \sum_{u \in \mathcal{V}_q} \lambda_u^{1-\alpha} \right)^{\frac{1}{1-\alpha}} & , \alpha > 0,\ \alpha \neq 1, \\ \left(\prod_{u \in \mathcal{V}_q} \lambda_u \right)^{\frac{1}{|\mathcal{V}_q|}} & , \alpha = 1, \end{cases} \tag{10}$$

where, α is the fairness parameter, λ_u is as defined in (6), and $\mathcal{V}_q$ is the set of users associated with the cluster q.

We define SINR coverage as the probability of a random user u receiving SINR $\gamma_{u,s}^m$ greater than the minimum SINR threshold in Table 2 from at least one sector s. Further, we define rate coverage as the probability of a random user u receiving rate λ_u greater than the rate threshold R. This rate threshold is a system parameter that can be controlled by the operator.

We consider the percentage of energy saved, represented by $\mathcal{E}$, as the metric for energy efficiency. For a given BSS pattern $\mathcal{Z}_{a1/a2}$ which means $a1$ out of $a2$ BSs are switched off, the percentage energy saving is

$$\mathcal{E} = \frac{a1}{a2} \times 100\,. \tag{11}$$

Next, we consider a snapshot based approach and consider a user realization for a given user density μ. We formulate the joint BSS and CoMP as an optimization problem for this user realization.

III. JOINT BSS AND COMP PROBLEM FORMULATION

We use w_b as a binary BSS variable to denote BS b in ON ($w_b = 0$) or OFF ($w_b = 1$) state. We focus on the cluster q in the center as depicted in Fig. 1. The power consumption of a BS b in idle and active state is given by P_{idle} and P_{tot}, respectively. Then, for a given user realization, to achieve energy efficiency, we should optimize the following objective function [26]

$$\min_{w_b} \sum_{b \in \mathcal{B}_q} w_b P_{idle}^b + (1 - w_b) P_{tot}^b\,. \tag{12}$$

The objective function in (12) simplifies to $\min_{w_b} \sum_{b \in \mathcal{B}_q} w_b (P_{idle}^b - P_{tot}^b)$. Given P_{idle}^b is always less than P_{tot}^b, for a homogeneous cellular environment, (12) is equivalent to $\max_{w_b} \sum_{b \in \mathcal{B}_q} w_b$. Let $x_{u,s}$ denote an association variable of user u with sector s such that $x_{u,s} \in \{0, 1\}$. Then, the BSS with CoMP problem can be framed as an optimization problem for a given user realization as follows.

We consider a maximum SINR based user association and its corresponding binary association variable as $x_{u,s}$. Based on this if any user u is associated to a sector s, this variable $x_{u,s}$ is set to 1, otherwise $x_{u,s}$ is set to 0. We use $z_{u,s}$ as a binary variable that denotes whether the user u associated to sector s will receive CoMP transmission from the virtual cluster k (such that $s \in \mathcal{S}_k$ and $z_{u,s}$=1) or will receive conventional downlink transmission from the sector s ($z_{u,s}$=0). We set the value of $z_{u,s}$ as 1 if the $\gamma_{u,s}^m$ is less than the CoMP SINR threshold Γ_d. Given the number of CoMP and non-CoMP users, the virtual cluster k has to decide the optimal CoMP time fraction θ_k. We define $\beta_{u,k}$ as the time fraction of θ_k for which an individual CoMP user u receives joint downlink transmission from the virtual cluster k. Further, any user in the center cluster q should obtain a rate higher than a predetermined rate threshold R with or without CoMP from corresponding virtual cluster k or sector s, respectively. Then, given the utility function in (7), the joint BSS with CoMP resource allocation and user scheduling problem for a cluster q can be formulated as the following optimization problem.

$$\mathbb{B} \quad : \quad \max_{\substack{w_b, \Gamma_d, \beta_{u,k}, \\ \beta_{u,s}, \theta_k}} \sum_{b \in \mathcal{B}_q} w_b \tag{13}$$

$$\text{s.t.} \quad \sum_{b \in \mathcal{B}_q} w_b \leq |\mathcal{B}_q| - 1\,, \tag{14}$$

$$w_b \in \{0, 1\},\ \forall b \in \mathcal{B}_q\,, \tag{15}$$

$$\lambda_u = \Big[\sum_{k \in \mathcal{K}_q} \sum_{s \in \mathcal{S}_k} (1 - \theta_k) x_{u,s} (1 - z_{u,s}) \beta_{u,s} r_{u,s} + \sum_{k \in \mathcal{K}_q} \sum_{s \in \mathcal{S}_k} \theta_k x_{u,s} z_{u,s} \beta_{u,k} r_{u,k} \Big],\ \forall u \in \mathcal{V}_q\,, \tag{16}$$

$$\lambda_u > R\ \forall u \in \mathcal{V}_q\,, \tag{17}$$

$$\gamma_{u,s}^m = \frac{(1 - w_{\lceil s/3 \rceil}) P_s^m h_{u,s}^m}{\sum_{\substack{\hat{s} \neq s \\ \hat{s} \in \mathcal{S}}} (1 - w_{\lceil \hat{s}/3 \rceil}) P_{\hat{s}}^m h_{u,\hat{s}}^m + \sigma^2}, \forall u \in \mathcal{V}_q, \forall s \in \mathcal{W}_q, \tag{18}$$

$$\gamma_{u,k}^m = \frac{\sum_{v \in \mathcal{S}_k} (1 - w_{\lceil v/3 \rceil}) P_v^m h_{u,v}^m}{\sum_{\substack{\hat{v} \in \mathcal{S} \\ \hat{v} \notin \mathcal{S}_k}} (1 - w_{\lceil \hat{v}/3 \rceil}) P_{\hat{v}}^m h_{u,\hat{v}}^m + \sigma^2}, \forall u \in \mathcal{V}_q, \forall k \in \mathcal{K}_q, \tag{19}$$

$$x_{u,s} = \begin{cases} 1, & \text{if } s = \arg\max_s \{\gamma_{u,s}^m\}, \\ 0, & \text{otherwise}, \forall u \in \mathcal{V}_q, \forall s \in \mathcal{W}_q, \end{cases} \tag{20}$$

$$z_{u,s} = \begin{cases} 1, & \text{if } \gamma_{u,s}^m \leq \Gamma_d x_{u,s},\ s \in \mathcal{S}_k,\ k \in \mathcal{K}_q, \\ 0, & \text{otherwise},\ \forall u \in \mathcal{V}_q, \forall s \in \mathcal{W}_q,\ |\mathcal{S}_k| > 1\,, \end{cases} \tag{21}$$

$$\sum_{s \in \mathcal{S}_k} \sum_{u \in \mathcal{U}_k} z_{u,s} x_{u,s} \beta_{u,k} \leq 1,\ \forall k \in \mathcal{K}_q\,, \tag{22}$$

$$\sum_{u \in \mathcal{U}_k} (1 - z_{u,s}) x_{u,s} \beta_{u,s} \leq 1,\ \forall s \in \mathcal{S}_k,\ \forall k \in \mathcal{K}_q\,, \tag{23}$$

$$\beta_{u,s} \geq 0,\ \forall u \in \mathcal{U}_k,\ \forall s \in \mathcal{S}_k,\ \forall k \in \mathcal{K}_q\,, \tag{24}$$

$$\beta_{u,k} \geq 0,\ \forall u \in \mathcal{U}_k,\ \forall k \in \mathcal{K}_q\,, \tag{25}$$

$$\theta_k \in [0, 1],\ \forall k \in \mathcal{K}_q\,, \tag{26}$$

$$\Gamma_d \in [\xi_{min}^d, \xi_{max}^d]\,, \tag{27}$$

where, the objective function in (13) ensures maximum energy savings, while, the constraint in (14) is to ensure that atleast one BS in the center cluster is in ON state, the constraint in (15) reflects that a BS can be either in ON

or OFF state, the constraint in (16) is the resultant rate of a user with joint BSS and CoMP, the constraint in (17) gives the condition that the resultant rate should be greater than the predetermined threshold R, the constraint in (18) is required to account for the change in SINR from a sector with BSS, the SINR from virtual cluster k is recomputed in the constraint in (19) as with BSS the received power from a sector v corresponding to BS $b = \lceil v/3 \rceil$ or received power from an interfering sector $\hat{v}$ can be zero if the corresponding BS is switched off, the constraint in (20) is required to re-compute user association with BSS through the additional term of $(1-w_b)$ that ensures the maximum SINR is computed only over the BSs that are still in ON state, the constraint in (21) ensures that a user is served as a CoMP user based on received SINR only from sectors of BSs still in ON state and for virtual cluster with more than one sector available for CoMP, the constraint in (22) indicates that time fractions of θ_k allocated to all CoMP users in cluster k must be less than equal to 1. Similarly, the constraint in (23) indicates that time fractions of $(1-\theta_k)$ allocated individually in each sector s to non-CoMP users must be less than equal to 1. The constraints in (24) and (25) are required to ensure non-negative time fractions for non-CoMP and CoMP users, respectively. The constraint in (26) ensures that the CoMP time fraction is not more than the total available time. The values of ξ^d_{min} and ξ^d_{max} in the constraint (27) define the permitted range for the CoMP threshold Γ_d.

Note that the optimization problem presented in (13) is an MINLP and the problem becomes more complex with increasing number of BSs, i.e., $|\mathcal{B}_q|$. Therefore, we decompose the joint problem of BSS and CoMP in (13) into purely a CoMP resource allocation and user scheduling problem in the next section, and use it to re-frame a simplified BSS with CoMP problem later.

IV. COMP PROBLEM FORMULATION

For the CoMP based system, we use $z_{u,s}$, and $x_{u,s}$ as binary variables as explained in the previous section. For a given user realization, this CoMP problem jointly determines the solution for the optimal resource fraction θ_k that can be allocated for CoMP users, the optimal time fraction scheduled for individual users, i.e., $\beta_{u,s}(1-\theta_k)$ fraction of time that can be allocated to a non-CoMP user u by a sector s, and $\beta_{u,k}\theta_k$ fraction of time that can be allocated to a CoMP user jointly from the sectors in the virtual cluster k. Then, given the utility function in (7), the joint CoMP resource allocation and user scheduling problem for a virtual cluster k can be formulated as the following optimization problem.

$$\mathbb{P} \quad : \quad \max_{\substack{\Gamma_d,\theta_k,\\ \beta_{u,s},\beta_{u,k}}} \sum_{u\in\mathcal{U}_k} \mathbb{U}_\alpha(\lambda_u)\,, \tag{28}$$

$$\text{s.t. } \lambda_u = (1-\theta_k)\sum_{s\in S_k} x_{u,s}(1-z_{u,s})\beta_{u,s}r_{u,s} + \theta_k \sum_{s\in S_k} x_{u,s}z_{u,s}\beta_{u,k}r_{u,k}, \ \forall u\in\mathcal{U}_k\,, \tag{29}$$

$$x_{u,s} = \begin{cases} 1, & \text{if } s = \arg\max_s\{\gamma^m_{u,s}\}, \\ 0, & \text{otherwise}, \forall u\in\mathcal{U}_k, \forall s\in\mathcal{S}_k\,, \end{cases} \tag{30}$$

$$z_{u,s} = \begin{cases} 1, & \text{if } \gamma^m_{u,s} \le \Gamma_d x_{u,s},\ s\in\mathcal{S}_k,\ |\mathcal{S}_k|>1, \\ 0, & \text{otherwise},\ \forall u\in\mathcal{U}_k, \forall s\in\mathcal{S}_k\,, \end{cases} \tag{31}$$

$$\sum_{s\in\mathcal{S}_k}\ \sum_{u\in\mathcal{U}_k} z_{u,s}x_{u,s}\beta_{u,k} \le 1\,, \tag{32}$$

$$\sum_{u\in\mathcal{U}_k} (1-z_{u,s})x_{u,s}\beta_{u,s} \le 1,\ \forall s\in\mathcal{S}_k\,, \tag{33}$$

$$\beta_{u,s} \ge 0,\ \forall u\in\mathcal{U}_k,\ \forall s\in\mathcal{S}_k\,, \tag{34}$$

$$\beta_{u,k} \ge 0,\ \forall u\in\mathcal{U}_k\,, \tag{35}$$

$$\theta_k \in [0,1]\,, \tag{36}$$

$$(1)\,,(27)\,,$$

where, the user rate is defined by (29) such that any non-CoMP users u gets a fraction of $\beta_{u,s}(1-\theta_k)$ from the sector s and any CoMP users u gets a fraction of $\beta_{u,k}\theta_k$ from all sectors in k, $x_{u,s}$ in (30) represents the maximum SINR based binary user association variable, the constraint in (31) implies that a user can be either CoMP or non-CoMP with corresponding binary $z_{u,s}$. The $r_{u,k}$ in (29) is given in (9).

The joint resource allocation and user scheduling problem in (28) is also an MINLP which is difficult to solve simultaneously for the multiple optimization variables (namely, Γ_d, θ_k, $\beta_{u,s}$, $\beta_{u,k}$). Hence, we next present propositions that provide optimal solutions with respect to $\beta_{u,s}$, $\beta_{u,k}$, and θ_k for a given Γ_d and $x_{u,s}$ in a virtual cluster k. This is a valid assumption as user association ($x_{u,s}$) is typically maximum SINR based and thresholds like Γ_d can be determined via simulations. We first present Proposition 1 which solves the user scheduling problem for any CoMP resource allocation (θ_k) because the user scheduling is independent θ_k.

Proposition 1: For a virtual cluster k, given any user association $x_{u,s}$, CoMP SINR threshold Γ_d, with at least one CoMP user u such that $\gamma^m_{u,s} \le \Gamma_d$, and any CoMP time fraction θ_k, the optimal time fraction of $(1-\theta_k)$, allocated by the α-Fair scheduler in any sector $s\in\mathcal{S}_k$ for a non-CoMP user u is equal to

$$\beta^*_{u,s} = \frac{\mathtt{t}_{u,s,\alpha}}{\sum\limits_{v\in\mathcal{U}_{nc,s}} \mathtt{t}_{v,s,\alpha}}\,, \forall s\in\mathcal{S}_k,\ \forall u\in\mathcal{U}_{nc}\,, \tag{37}$$

where, $\mathtt{t}_{u,s,\alpha} = r^{\frac{1-\alpha}{\alpha}}_{u,s}$, and the optimal time fraction of θ_k allocated by an α-Fair scheduler for all the sectors jointly to a CoMP user u is equal to

$$\beta^*_{u,k} = \frac{\mathtt{t}_{u,k,\alpha}}{\sum\limits_{v\in\mathcal{U}_c} \mathtt{t}_{v,k,\alpha}},\ \forall u\in\mathcal{U}_c\,, \tag{38}$$

where, $\mathtt{t}_{u,k,\alpha} = r^{\frac{1-\alpha}{\alpha}}_{u,k}$, $\mathcal{U}_c = \{1,2,...U_c\}$, $\mathcal{U}_{nc} = \{1,2,...U_{nc}\}$, and $\mathcal{U}_{nc,s} = \{1,2,...U_{nc,s}\}$ denote the set of CoMP users in $\mathcal{S}_k$, the set of non-CoMP users in $\mathcal{S}_k$, and the set of non-CoMP users in any sector $s\in\mathcal{S}_k$ in the virtual cluster, respectively.

Proof: For any given user association $x_{u,s}$ (note that it need not be maximum SINR based) and CoMP SINR threshold Γ_d, the virtual cluster k can compute $z_{u,s}$ using (31). Given binary

This article has been accepted for publication in a future issue of this journal, but has not been fully edited. Content may change prior to final publication. Citation information: DOI 10.1109/ACCESS.2017.2783398, IEEE Access

$z_{u,s}$, a user u can be classified as CoMP or non-CoMP user into the sets $\mathcal{U}_c$ or $\mathcal{U}_{nc}$, respectively. Further, the set of non-CoMP users for every sector $s \in \mathcal{S}_k$, denoted by $\mathcal{U}_{nc,s}$, can be obtained. Then, as $\mathcal{U}_k = \mathcal{U}_c \cup \mathcal{U}_{nc}$, the objective function in (28) denoted by $\mathbb{Y}$ can be represented as

$$\mathbb{Y} = \sum_{u\in\mathcal{U}_k} \frac{\lambda_u^{1-\alpha}}{1-\alpha} = \sum_{u\in\mathcal{U}_{nc}} \frac{\lambda_u^{1-\alpha}}{1-\alpha} + \sum_{u\in\mathcal{U}_c} \frac{\lambda_u^{1-\alpha}}{1-\alpha}, \tag{39}$$

which using (29) becomes

$$\mathbb{Y} = \sum_{u\in\mathcal{U}_{nc}} \sum_{s\in S_k} x_{u,s} \frac{(1-\theta_k)^{1-\alpha}(r_{u,s}\beta_{u,s})^{1-\alpha}}{1-\alpha} + \sum_{u\in\mathcal{U}_c} \sum_{s\in S_k} x_{u,s} \frac{\theta_k^{1-\alpha}(r_{u,k}\beta_{u,k})^{1-\alpha}}{1-\alpha}.$$

Then, for any given θ_k, $x_{u,s}$, and Γ_d, the optimization problem in (28) can be simplified to

$$\mathbb{P}^* : \max_{\beta_{u,s},\beta_{u,k}} \mathbb{Y} \tag{40}$$

$$\text{s.t.} \sum_{u\in\mathcal{U}_{nc,s}} \beta_{u,s} \le 1, \ \forall s \in \mathcal{S}_k, \tag{41}$$

$$\sum_{u\in\mathcal{U}_c} \beta_{u,k} \le 1, \tag{42}$$

$$(34), \text{ and } (35),$$

where, (41) and (42) are obtained from (22) and (23), respectively. The Lagrangian function of (40) can be defined as

$$\mathbf{L}(\mathbb{Y}, \mathbb{V}_s, \mathbb{V}_k, \mathbb{X}_{u,s}, \mathbb{X}_{u,k}) = -\mathbb{Y} + \sum_{s\in\mathcal{S}_k} \mathbb{V}_s \left(\sum_{u\in\mathcal{U}_{nc,s}} \beta_{u,s} - 1 \right) + \mathbb{V}_k \left(\sum_{u\in\mathcal{U}_c} \beta_{u,k} - 1 \right) - \sum_{s\in\mathcal{S}_k} \sum_{u\in\mathcal{U}_{nc,s}} \mathbb{X}_{u,s}\beta_{u,s} - \sum_{u\in\mathcal{U}_c} \mathbb{X}_{u,k}\beta_{u,k}, \tag{43}$$

where, $\mathbb{V}_s$, $\mathbb{V}_k$, $\mathbb{X}_{u,s}$, and $\mathbb{X}_{u,k}$ are the KKT multipliers [24] for (41), (42), (34), and (35), respectively. Considering the complementary slackness KKT conditions, the values of $\mathbb{X}_{u,s}$ and $\mathbb{X}_{u,k}$ turn out to be zero for a user u whenever it receives non-zero $\beta_{u,s}$ or $\beta_{u,k}$ from a sector s or a cluster k, respectively. Thus, the corresponding (43) for users receiving non-zero rate (i.e., $x_{u,s}$=1) becomes

$$\mathbf{L}(\mathbb{Y}, \mathbb{V}_s, \mathbb{V}_k) = -\mathbb{Y} + \sum_{s\in\mathcal{S}_k} \mathbb{V}_s \left(\sum_{u\in\mathcal{U}_{nc,s}} \beta_{u,s} - 1 \right) + \mathbb{V}_k \left(\sum_{u\in\mathcal{U}_c} \beta_{u,k} - 1 \right). \tag{44}$$

The first-order stationarity conditions of (44) for (41) and (42) result in

$$\frac{d\mathbf{L}}{d\beta_{u,s}} = -\left[(1-\theta_k) r_{u,s}\right]^{1-\alpha} \beta_{u,s}^{-\alpha} + \mathbb{V}_s = 0 \text{ and} \tag{45}$$

$$\frac{d\mathbf{L}}{d\beta_{u,k}} = -\left[\theta_k r_{u,k}\right]^{1-\alpha} \beta_{u,k}^{-\alpha} + \mathbb{V}_k = 0, \text{ respectively.} \tag{46}$$

Solving (45) and (46) jointly with (41) and (42) result in (37) and (38), respectively. This completes the proof of *Proposition* 1. ■

TABLE 3: Various values of α and corresponding θ_k^* for a virtual cluster k.

α	δ	θ_k^*
1	$\frac{N_c}{N_{nc}}$	$\frac{N_c}{N_c+N_{nc}}$
2	$\sqrt{\left[\frac{\sum_{u\in\mathcal{U}_c}(r_{u,k}\beta_{u,k}^*)^{-1}}{\sum_{u\in\mathcal{U}_{nc}}\sum_{s\in S_k} x_{u,s}(r_{u,s}\beta_{u,s}^*)^{-1}}\right]}$	$\frac{\delta}{1+\delta}$
α	$\sqrt{\left[\frac{\sum_{u\in\mathcal{U}_c}(r_{u,k}\beta_{u,k}^*)^{1-\alpha}}{\sum_{u\in\mathcal{U}_{nc}}\sum_{s\in S_k} x_{u,s}(r_{u,s}\beta_{u,s}^*)^{1-\alpha}}\right]}$	$\frac{\delta}{1+\delta}$

Note that for $\alpha = 1$, i.e., a proportional fair scheduler, (37) and (38) result in time fractions $1/N_{nc,s}$ and $1/N_c$ for Non-CoMP and CoMP users, respectively, in any sector s of the CoMP cluster. The result presented in (37) and (38) gives the time fraction allocated to the set of users $\mathcal{U}_k$ in the cluster k. It is observed from (37) that the time fraction allocated for a non-CoMP user u depends only on the non-CoMP users in the sector s. Further, (38) presents the time fraction allocated for a CoMP user u in the virtual cluster k which depends on all CoMP users in the same virtual cluster k. Next in Proposition 2, we present optimal resource allocation of CoMP users for the α-Fair scheduler.

Proposition 2: For a given user association $x_{u,s}$ and CoMP SINR threshold Γ_d, the optimal time fraction θ_k^* for CoMP users in a virtual cluster k is given by

$$\theta_k^* = \frac{\delta}{1+\delta}, \tag{47}$$

where,

$$\delta = \left[\frac{\sum_{u\in\mathcal{U}_c}(r_{u,k}\beta_{u,k}^*)^{1-\alpha}}{\sum_{u\in\mathcal{U}_{nc}}\sum_{s\in S_k} x_{u,s}(r_{u,s}\beta_{u,s}^*)^{1-\alpha}} \right]^{\frac{1}{\alpha}}, \tag{48}$$

with $\beta_{u,s}^*$ and $\beta_{u,k}^*$ as in (37) and (38), respectively.

Proof: For any given user association $x_{u,s}$ and CoMP SINR threshold Γ_d, the virtual cluster k can be classify users into the sets $\mathcal{U}_c$ or $\mathcal{U}_{nc}$ as shown in the proof of Proposition 1. Then, as $\mathcal{U}_k = \mathcal{U}_c \cup \mathcal{U}_{nc}$, the objective function in (28) can be represented as

$$\sum_{u\in\mathcal{U}_k} \frac{\lambda_u^{1-\alpha}}{1-\alpha} = \sum_{u\in\mathcal{U}_{nc}} \frac{\lambda_u^{1-\alpha}}{1-\alpha} + \sum_{u\in\mathcal{U}_c} \frac{\lambda_u^{1-\alpha}}{1-\alpha},$$

which given $x_{u,s}$ is binary, (29), (37), and (38) becomes

$$\sum_{u\in\mathcal{U}_{nc}} \sum_{s\in S_k} x_{u,s} \frac{(1-\theta_k)^{1-\alpha}(r_{u,s}\beta_{u,s}^*)^{1-\alpha}}{1-\alpha} + \sum_{u\in\mathcal{U}_c} \frac{\theta_k^{1-\alpha}(r_{u,k}\beta_{u,k}^*)^{1-\alpha}}{1-\alpha}. \tag{49}$$

Differentiating (49) with respect to θ_k and equating to 0 gives

$$(1-\theta_k^*)^{-\alpha} \sum_{u\in\mathcal{U}_{nc}} \sum_{s\in S_k} x_{u,s}(r_{u,s}\beta_{u,s}^*)^{1-\alpha} = (\theta_k^*)^{-\alpha} \sum_{u\in\mathcal{U}_c} (r_{u,k}\beta_{u,k}^*)^{1-\alpha},$$

which on simplification results in (47). This completes the proof of *Proposition* 2. ■

This article has been accepted for publication in a future issue of this journal, but has not been fully edited. Content may change prior to final publication. Citation information: DOI 10.1109/ACCESS.2017.2783398, IEEE Access

The result presented in (47) is valid for any α-Fair scheduler. Further, it is observed from (47) that the optimal time fraction for CoMP users θ_k^* depends on the set of all users $\mathcal{U}_k$ in the virtual cluster k irrespective of whether it is CoMP or non-CoMP. The optimal CoMP time fraction θ_k^* for some commonly used α-Fair schedulers is presented in Table 3. Note that for a proportional fair scheduler ($\alpha = 1$), θ_k^* is independent of the user link rates and the time allocated to each user. In Table 3, the N_{nc} and N_c in a virtual cluster k are given by

$$N_{nc} = \sum_{s\in\mathcal{S}_k}\sum_{u\in\mathcal{U}_k}(1-z_{u,s})x_{u,s}, \text{ and} \tag{50}$$

$$N_c = \sum_{u\in\mathcal{U}_k}\sum_{s\in\mathcal{S}_k} z_{u,s}x_{u,s}, \text{ respectively.} \tag{51}$$

Next, we present a re-framed and simplified BSS with CoMP optimization problem for the center cluster q.

V. BSS WITH COMP

The simplified problem of BSS with CoMP for a given Γ_d, and the optimal $\beta_{u,s}$, $\beta_{u,k}$, and θ_k obtained from (37), (38), and (47), respectively, is formulated as follows

$$\mathbb{B}^* \quad : \quad \max_{w_b} \sum_{b\in\mathcal{B}_q} w_b \tag{52}$$

$$\text{s.t.} \quad (14), (15), (18), (19), (20), (21)$$

$$\lambda_u = \Big[\sum_{k\in\mathcal{K}_q}\sum_{s\in\mathcal{S}_k}(1-\theta_k^*)x_{u,s}(1-z_{u,s})\beta_{u,s}^* r_{u,s} + \sum_{k\in\mathcal{K}_q}\sum_{s\in\mathcal{S}_k}\theta_k^* x_{u,s}z_{u,s}\beta_{u,k}^* r_{u,k}\Big], \ \forall u\in\mathcal{V}_q, \tag{53}$$

$$\lambda_u > R, \ \forall u\in\mathcal{V}_q, \tag{54}$$

$$\beta_{u,s}^* \quad \text{is as in (37)}, \forall u\in\mathcal{V}_q, \ \forall s\in\mathcal{W}_q, \tag{55}$$

$$\beta_{u,k}^* \quad \text{is as in (38)}, \forall u\in\mathcal{U}_k, \ \forall k\in\mathcal{K}_q, \tag{56}$$

$$\theta_k^* \quad \text{is as in (47)}, \ \forall k\in\mathcal{K}_q, \tag{57}$$

where, the objective function in (52) is the same as in (13), the constraints (14), (15), (18)–(21) are required as in (13). However, (53) which is the resultant rate of a user with BSS and CoMP is now computed using $\beta_{u,s}^*$, $\beta_{u,k}^*$, and θ_k^* from (55), (56), and (57), that are obtained using (37), (38), and (47), respectively. Further, the constraint in (54) is as in (17) to ensure that each user's rate is above the predetermined rate threshold R. Note that although the optimization problem presented in (52) is relatively simpler than (13), it is still an MINLP. Hence, we next present a heuristic that solves the BSS with CoMP optimization problem.

VI. PROPOSED DYNAMIC HEURISTIC FOR BSS WITH COMP

In this section, we present a dynamic heuristic that selects the optimum BSS pattern for a pre-determined set of virtual clusters that perform CoMP in the center cluster q. An efficient BSS algorithm should avoid frequent switching on/off and ping-pong effect to protect the equipment from damage

Algorithm 1 Dynamic Base Station Sleeping with CoMP

INPUTS : $\{P_s^m(t)h_{u,s}^m(t)\}$, $\mathcal{V}_q(t)$, Γ_d, R, $\{\mathcal{Z}_{a1/a2}^j\}$, τ, $\{\Lambda_j^{min}(t-1)\}, \{\Lambda_j^{min}(t-2)\}, \ldots, \{\Lambda_j^{min}(t-\tau)\}$
OUTPUTS : $\mathcal{Z}_{a1/a2}^*$, $\{\Lambda_j^{min}(t)\}$
Sort $\mathcal{Z}_{a1/a2}$ in decreasing order of energy consumption
Initialize : $J = |\{\mathcal{Z}_{a1/a2}^j\}|$, $\mathcal{Z}_{a1/a2}^* = \mathcal{Z}_{a1/a2}^1$, j=1
Repeat
  Initialize : u=1, $\{z_{u,s}\} = 0$
  Repeat
    Sort $\{P_s^m(t)h_{u,s}^m(t)\}$ in decreasing order and set $x_{u,s}(t) = 1$
    $\gamma_{u,s}^m(t) = f(\{P_s^m(t)h_{u,s}^m(t)\})$ as in (18)
    if $\gamma_{u,s}^m(t) \le \Gamma_d$ **then**
      $\gamma_{u,k}^m(t) = f(\{P_s^m(t)h_{u,s}^m(t)\})$ as in (19)
      $z_{u,s}(t) = 1$
    else
      $z_{u,s}(t) = 0$
    end if
    Set $u = u + 1$
  Until $u > |\mathcal{V}_q(t)|$
  Set u=1
  Repeat
    Compute $\lambda_u(t)$ as in (58)
    Set $u = u + 1$
  Until $u > |\mathcal{V}_q(t)|$
  Compute $\Lambda_j^{min}(t)$ as in (59)
  if $\left\lfloor \frac{\sum_{n=t-\tau}^{t}\Lambda_j^{min}(n)}{\tau} \right\rfloor > R$ **then**
    $\mathcal{Z}_{a1/a2}^* = \mathcal{Z}_{a1/a2}^j$
  end if
  Set $j = j + 1$
Until $j > J$
Stop

[3]. Hence, instead of making BSS decisions over instantaneous parameters, we propose to use values averaged over τ samples. Thus, the proposed heuristic selects the optimum BSS pattern based on the minimum rate of users in the CoMP cluster, averaged over τ samples. This ensures that the BSS decision is not only based on the instantaneous minimum rate but also considers the averaged value over τ samples. Thereby, avoiding frequent switching on/off and ping-pong effect based on τ.

Let t denote the current instance of time. Then, the proposed heuristic assumes that the set of users at time instance t, denoted by $\mathcal{V}_q(t)$, and the set of received powers for any user u from any sector s at time instance t, represented by $\{P_s^m(t)h_{u,s}^m(t)\}$ are available. The heuristic considers a set of BSS patterns denoted by $\{\mathcal{Z}_{a1/a2}^j\}$. Note that any element $\mathcal{Z}_{a1/a2}^j$ of this set is equivalent to a unique combination of $\{w_b\}$, the binary BSS indicator variables specified in (15). The heuristic also takes Γ_d and R as an input. The user rate for a

This article has been accepted for publication in a future issue of this journal, but has not been fully edited. Content may change prior to final publication. Citation information: DOI 10.1109/ACCESS.2017.2783398, IEEE Access

time instance t is computed as

$$\lambda_u(t) = \sum_{k\in\mathcal{K}_q}\sum_{s\in\mathcal{S}_k}(1-\theta_k^*(t))x_{u,s}(t)(1-z_{u,s}(t))\beta_{u,s}^*(t)r_{u,s}(t) + \sum_{k\in\mathcal{K}_q}\sum_{s\in\mathcal{S}_k}\theta_k^*(t)x_{u,s}(t)z_{u,s}(t)\beta_{u,k}^*(t)r_{u,k}(t),\ \forall u\in\mathcal{V}_q(t), \quad (58)$$

where, $\theta_k^*(t)$ is the optimal time fraction for CoMP (47) that depends on the set of users $\mathcal{V}_q(t)$ at the time instance t, $x_{u,s}(t)$ denotes the association of user u with sector s, $z_{u,s}(t)$ is the CoMP variable of user u with the virtual cluster k, $\beta_{u,s}^*(t)$ and $\beta_{u,k}^*(t)$ are the optimal CoMP and non-CoMP users time fractions, respectively. Similarly, $r_{u,s}(t)$ and $r_{u,k}(t)$ are the link rates of CoMP and non-CoMP users, respectively. Please note that the variables are same as explained in the Section III except that now their value can vary with respect to the time instance t under consideration.

We define the minimum user rate in the CoMP cluster q for the j^{th} BSS pattern as follows,

$$\Lambda_j^{min}(t) = \min_{u\in\mathcal{V}_q(t)}\{\lambda_u(t)\}. \quad (59)$$

The heuristic requires the value of these minimum rates for the various patterns over τ samples. Thus, the vectors $\{\Lambda_j^{min}(t-1)\}, \{\Lambda_j^{min}(t-2)\}, \ldots, \{\Lambda_j^{min}(t-\tau)\}$ are also given as inputs to the proposed heuristic. Their values can be taken as zero for initialization. However, once the dynamic heuristic starts running, it computes $\{\Lambda_j^{min}(t)\}$ using (59) which are used for future iterations of the proposed heuristic.

Given the preceding initial values, the set of BSS patterns is first sorted in a decreasing order of energy consumption such that any BSS pattern $\{\mathcal{Z}_{a1/a2}^{j}\}$ consumes more than equal to the energy consumed by $\{\mathcal{Z}_{a1/a2}^{j+1}\}$. The heuristic starts with most energy consuming BSS pattern, i.e., all ON state. Next, the set of received powers $\{P_s^m(t)h_{u,s}^m(t)\}$ is sorted for any user u from all sectors s at time instant t. Using this operation at time instant t, for every user u, the sector s from which it receives maximum power is identified and $x_{u,s}(t)$ is set as 1. Next, given R it is decided whether a user u is a CoMP or a non-CoMP user. Then, for the BSS pattern under consideration, the received SINRs from the corresponding sector or virtual cluster is computed using (18) or (19), respectively. Note that (18) and (19) consider only the BSs that are still in ON state for the SINR calculations. In a separate loop over the number of users, i.e., $|\mathcal{V}_q(t)|$, the rate of each user is computed using (58).

Given the computation of each user's rate for the BSS pattern under consideration, the minimum user rate for the CoMP cluster is computed using (59). This value along with the previous $\tau-1$ values for the BSS pattern j are averaged over and compared with the rate threshold R. In case the minimum rate averaged over τ samples is higher than the rate threshold R then the heuristic selects this BSS pattern as the optimum pattern. Next, the number of switched off BSs is increased and the described steps are repeated until a BSS pattern is reached that no more satisfies the minimum rate constraint. The heuristic runs till either a optimum BSS pattern is obtained or gives the initial all ON state along with the $\{\Lambda_j^{min}(t)\}$ for various BSS patterns as an output. The heuristic is presented as a pseudo-code in Algo. 1.

The practical implementation of the proposed heuristic will run at any one of the BSs in a cluster q, such that this particular BS acts as a centralized controller and takes the decisions for all the BSs in the cluster. Given a user realization, the centralized controller decides whether CoMP should be performed or not based on the operator's rate threshold, and CoMP SINR threshold. The user's information particularly SINR and rate has to be sent to the centralized controller so that it can decide the CoMP configuration, CoMP time fraction, and user scheduling time fractions. This will result in additional overhead on the backhaul which can be compensated in terms of improvement in coverage and energy savings. Please note that the overhead for backhaul in terms of energy consumption during information exchange with centralized controller is negligible in the presence of fiber backhaul. The computational complexity of the proposed heuristic for every user realization is $O(J(|\mathcal{V}_q||\mathcal{B}_q| + |\mathcal{V}_q|))$. Note that worst case J is equal to $2^{|\mathcal{B}_q|}$. However, in practice, operators can optimize and choose from a lower number of BSS patterns. For example, in the numerical results presented next, we consider J equal to five BSS patterns. Further, the value of τ has to be carefully selected as a lower value of τ increases the frequency of BS switching on/offs per day leading to BS equipment damage and a higher value results in lower than expected energy savings.

TABLE 4: Simulation Parameters

B	49
Inter-site Distance	500 m
Penetration loss (υ)	20 dB
Loss due to Log-normal shadowing (ρ)	Standard deviation of 8 dB
P_{BS}	46 dBm
σ^2	2.2661e-15
PL(d)	136.8245+(39.086($\log_{10}$d-3)) [25]
M	99
Subchannel Bandwidth	180 kHz
SC_{OFDM}	12
SY_{OFDM}	14
$T_{Subframe}$	1 ms
Cluster size	7

VII. NUMERICAL RESULTS

We consider a center cluster with 7 BSs. To model the interference suitably, we consider a wrap-around system with 6 clusters of 7 BS each around the center cluster. We consider the simulation parameters specified by 3GPP for an urban homogeneous cellular environment as given in [25]. Thus, a total of 49 BSs are considered for simulations with inter-site distance of 500 m. The users are distributed uniformly randomly with the appropriate user density (μ) over the entire simulations area. We consider 100 user location realizations. For each location realization the results are averaged over 50 independent fading realizations. The simulation parameter

This article has been accepted for publication in a future issue of this journal, but has not been fully edited. Content may change prior to final publication. Citation information: DOI 10.1109/ACCESS.2017.2783398, IEEE Access

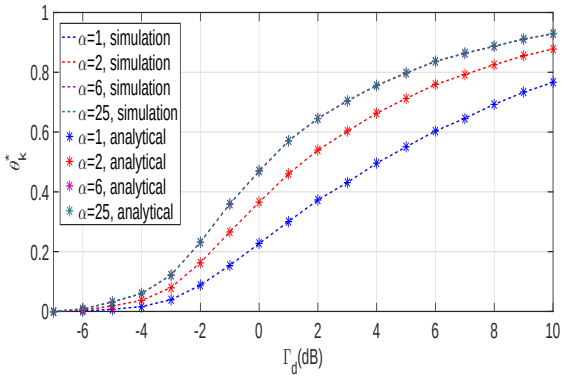

FIGURE 4: Variation of optimal CoMP time fraction (θ_k^*) with respect to CoMP SINR threshold (Γ_d) for various fairness parameter (α).

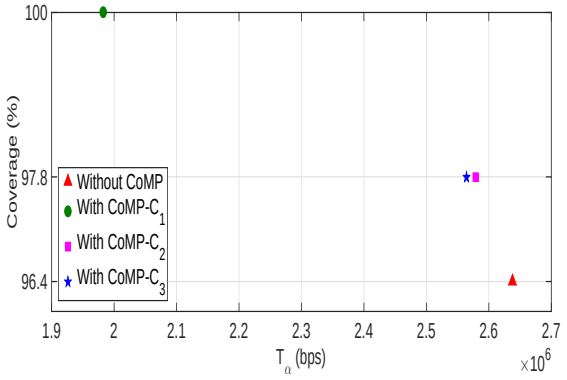

FIGURE 6: Coverage and throughput trade-off for user density of $60/km^2$ and BSS pattern $\mathcal{Z}_{3/7}$.

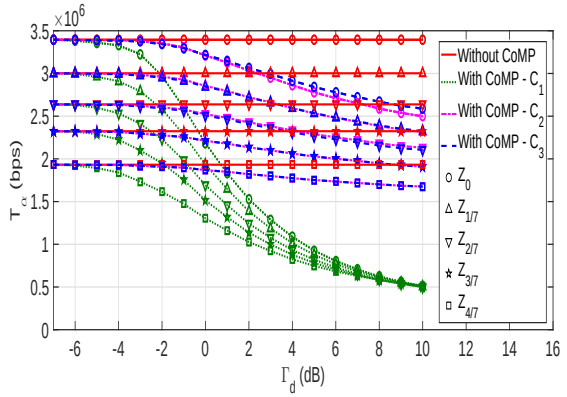

FIGURE 5: Variation of system throughput (T_α) with respect to CoMP SINR threshold (Γ_d), with and without CoMP, for various BSS patterns.

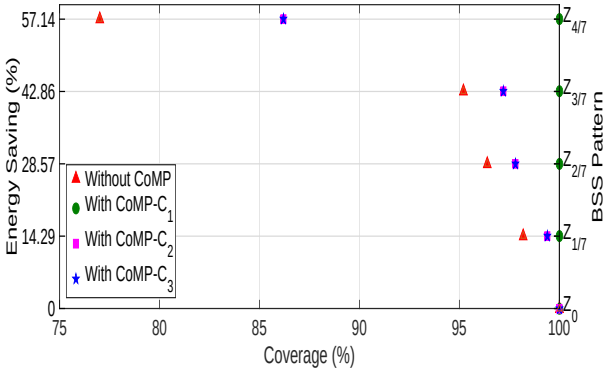

FIGURE 7: Energy and coverage trade-off for user density of $60/km^2$, various BSS patterns, and CoMP configurations (Note that the corresponding throughput is depicted in Fig. 8).

details are given in Table 4. To study the impact of change in μ over the system performance, we vary the average user density from 20 to 160 users per km^2.

The variation of θ_k^* with respect to Γ_d is shown in Fig. 4 for various values of α. Note that the optimal value of θ_k obtained via exhaustive search in simulations matches with the θ_k^* derived in (47). Further, the optimal CoMP time fraction increases with an increase in the CoMP SINR threshold as more number of users become CoMP users with increase in Γ_d. The increase in α values makes the α-Fair scheduler allocate more resources to edge users. Hence, an increase in the fairness parameter α results in an increase in θ_k^* for the same value of Γ_d. The increased θ_k^* ensures that the edge users (with SINR $\leq \Gamma_d$) will be served as CoMP users and receive more downlink time fraction.

The throughput metric corresponding to a $\alpha-$Fair scheduler is given in (10). The variation of T_α with respect to Γ_d, different BSS patterns, and $\alpha = 1$ is presented in Fig. 5. Note that the throughput decreases as more BSs are switched off. Further, even with various BSS patterns, the without CoMP scenario, CoMP configuration C_3, C_2, and C_1 are in decreasing order of throughput. This is due to the rate and coverage trade-off between these configurations. To better illustrate this, we present the rate and coverage trade-off for the BSS pattern $\mathcal{Z}_{3/7}$ in Fig. 6 for the user density of 60 users/km^2. The probability of coverage is as defined in Section IIF for SINR coverage. Note that an operator can run the network without CoMP for maximum throughput at the cost of coverage. On the other hand, all sectors CoMP in C_1 can provide maximum coverage at the cost of throughput.

The trade-off between percentage energy savings and coverage is presented for $\mathcal{Z}_0$ (all BSs in ON state) and BSS patterns $\mathcal{Z}_{1/7}$, $\mathcal{Z}_{2/7}$, $\mathcal{Z}_{3/7}$ and $\mathcal{Z}_{4/7}$, and various modes of CoMP operations in Fig. 7. The results considered are for

This article has been accepted for publication in a future issue of this journal, but has not been fully edited. Content may change prior to final publication. Citation information: DOI 10.1109/ACCESS.2017.2783398, IEEE Access

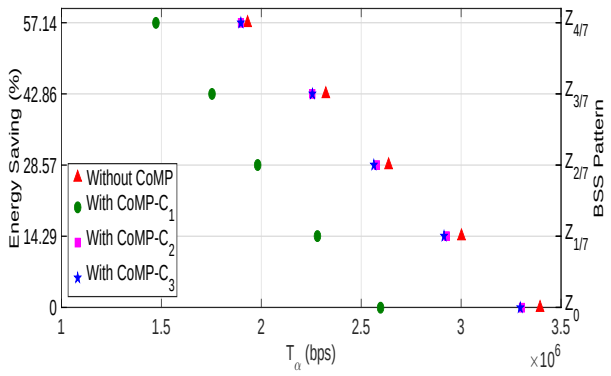

FIGURE 8: Energy and throughput trade-off for user density of $60/km^2$, various BSS patterns, and CoMP configurations.

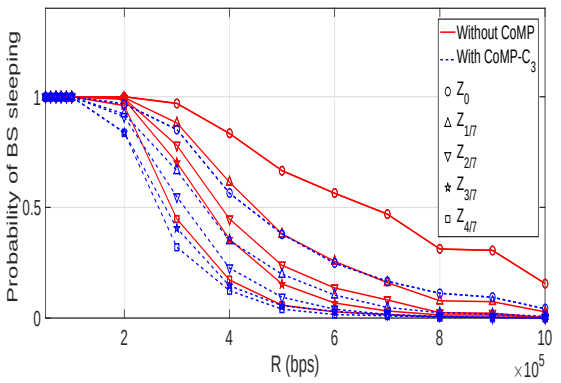

FIGURE 9: Variation of rate coverage with respect to rate threshold (R), for various BSS patterns in configuration C_3, $\alpha = 1$, and $\Gamma_d = -1$ dB.

BSS patterns shown in Fig. 3b, 3d, 3h, and 3i. An increase in the number of switched off BSs results in decrease in the coverage probability for any particular CoMP configuration. However, switching off BSs also increases the percentage energy savings. Thus, an operator can use the results in Fig. 7 to select the appropriate point of operation and the corresponding trade-off between percentage energy savings and coverage.

The corresponding energy and throughput trade-off for the various BSS patterns and CoMP modes in Fig. 7 is presented in Fig. 8. Note that an operator should jointly utilize the Fig. 7 and Fig. 8. For example, in Fig. 7, the coverage probability of C_1 is higher than C_2 for all BSS scenarios. Whereas, in Fig. 8, the throughput of C_1 is lower than C_2 for all BSS scenarios. Thus, multiple configurations of BSS with CoMP can be used to achieve various trade-offs between energy, coverage and rate trade-off which a traditional without CoMP system does not offer.

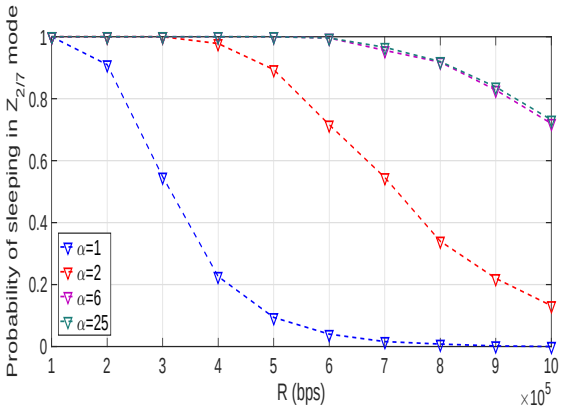

FIGURE 10: Variation of rate coverage with respect to rate threshold (R), for various α, BSS pattern $\mathcal{Z}_{2/7}$ in configuration C_3, and $\Gamma_d = -1$ dB.

For the next two set of results, we focus on C_3 as it results in least loss in throughput in comparison to without CoMP scenario. The rate coverage as defined in Section IIF is presented in Fig. 9 and Fig. 10 for $\alpha = 1$ and $\Gamma_d = -1dB$. In Fig. 9, the probability to operate in with a BSS pattern while ensuring the user rates to be higher than the rate threshold R is presented for without CoMP and with CoMP configuration C_3. The Fig. 9 shows that to maintain the same rate coverage with larges energy savings the system has to reduce the rate threshold R. Further, for the same R, BSS patterns with higher energy savings are less probable. Note that Fig. 10 is for BSS pattern $\mathcal{Z}_{2/7}$. It is observed from Fig. 10 that the probability for selecting the BSS pattern increases with increase in α. Thus, Fig. 9 and Fig. 10 also depict the rate-coverage and energy trade-off discussed earlier from a probabilistic perspective.

In Fig. 11, the variation of percentage energy saved from the proposed dynamic heuristic from Section VI for various time samples is presented. We select R as 0.2 Mbps. A snapshot of traffic profile variation is selected such that the user density variation in Fig. 11 is equivalent to the user traffic variation as considered in [3]. This simulation is carried out for 570 discrete instances of time per day. Thus, each sample corresponds to 2.5 minutes. The Fig. 11 shows the user density variation with respect to number of samples. The interval for averaging, τ, is taken as 20 discrete instances which is approximately 50 minutes. The maximum energy savings are obtained when the user density is the lowest. Further, due to the averaging over τ in the proposed heuristic, the BSS as seen through the changes in percentage energy saved in Fig. 11 do not exhibit the ping-pong effect or frequent switching on/offs even in the presence of rapidly varying user density.

To analyze the trade-off between energy efficiency and the number of BS switching on/offs per day, the average percentage energy saved per day along with the number of BS

This article has been accepted for publication in a future issue of this journal, but has not been fully edited. Content may change prior to final publication. Citation information: DOI 10.1109/ACCESS.2017.2783398, IEEE Access

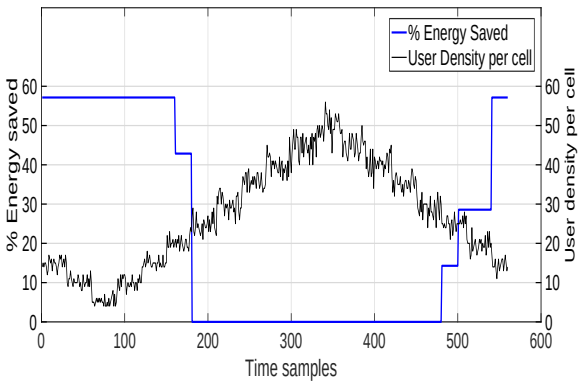

FIGURE 11: Variation of percentage energy saved for the proposed heuristic with respect to time for varying user density (averaged over $\tau = 20$ samples ≈ 50 minutes).

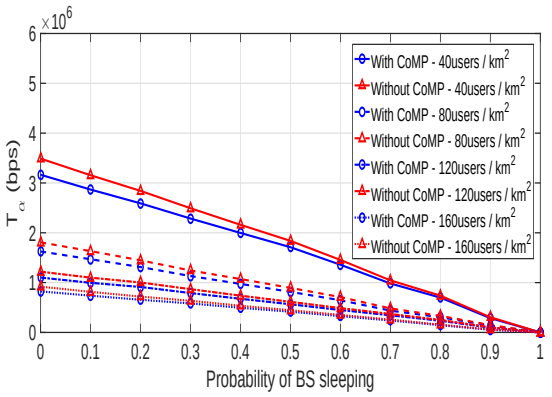

FIGURE 12: Variation of system throughput (T_α) with respect to probability of sleeping with and without CoMP, for various user densities and PPP based BS distribution.

TABLE 5: Percentage energy saved and number of BS switching on/offs per day for various values of τ.

No. of samples (τ) for averaging	Average percentage energy saved (%)	No. of BS switching on/offs per day
1	23.684	152
2	17.92	62
5	13.659	20
10	12.381	11
20	11.629	5
30	11.504	5
40	11.504	4
50	11.504	3
100	11.353	1
200	11.253	1

switching on/offs for various values of τ have been presented in Table 5. The value of τ is varied from 1 ($\approx$ 2.5 minutes) to 200 ($\approx$ 8 hours). As τ increases, the proposed heuristic makes a decision over larger number of time samples. Thus, with increasing τ, the average percentage energy saved decreases due to decreased number of switching on/offs per day. Hence, there exist a trade-off between energy efficiency and equipment life that can be achieved by selecting the appropriate value of τ.

To evaluate the performance of the proposed scheme for randomly distributed BSs, we also considered Poisson point process (PPP) based distribution of BSs as in [7], [13], [17]. For the following results, we performed BSS with CoMP using the proposed algorithm with a cluster size of 3. The average BS density of 5 BSs/km^2 was considered as in [17]. We also considered PPP distributed users with average user density varying from 20 to 160 users/km^2 while the probability of randomly switching off BSs was varied from 0 to 1. The presented results are generated after averaging over 50000 realizations consisting of 100 BS locations, 100 user locations, and 50 fading realizations. The variation of throughput with respect to probability of switching off of BSs is presented in Fig. 12 for various user densities. From Fig. 12, it is observed that the proposed algorithm for BSS with CoMP works even with randomly distributed BSs. Further, as in case of BSs arranged in the hexagonal grid, even for PPP distributed BSs, CoMP results in a decrease in throughput. Additionally, there exists a trade-off between energy savings and throughput that can be achieved by suitably selecting the point of operation for BSS with CoMP. The variation of system throughput with respect to CoMP SINR threshold for configuration C_1 for a PPP based model is presented in Fig. 13. The Fig. 13 shows that even for a PPP based system, the proposed algorithm performs similar to a hexagonal system as shown in Fig. 5 for various CoMP thresholds.

VIII. CONCLUSION

We have shown that loss in SINR coverage due to BSS can be compensated by CoMP transmission. We have formulated the joint BSS and CoMP problem as an optimization problem. The optimal solutions for a decomposed CoMP resource allocation and user scheduling problem have been derived. The derived results hold for arbitrary BSS patterns, and given a BSS pattern can also be applied to any cluster. The derived results have been used to formulate a simplified BSS with CoMP problem. A heuristic has been presented that solves the BSS with CoMP problem dynamically. Through numerical results it has been shown that the derived results match closely with simulations. Further, we have shown that BSS with CoMP can be used to achieve various possible trade-offs in energy savings, coverage, and throughput in both hexagonal and PPP based BSs. In future, the presented work will be extended with analysis on overhead in terms of cost, energy, and backhaul requirement for the CoMP enabled BSS system. Further, the upcoming scenario of multi-user CoMP with optimal resource allocation will also be considered in future.

This article has been accepted for publication in a future issue of this journal, but has not been fully edited. Content may change prior to final publication. Citation information: DOI 10.1109/ACCESS.2017.2783398, IEEE Access

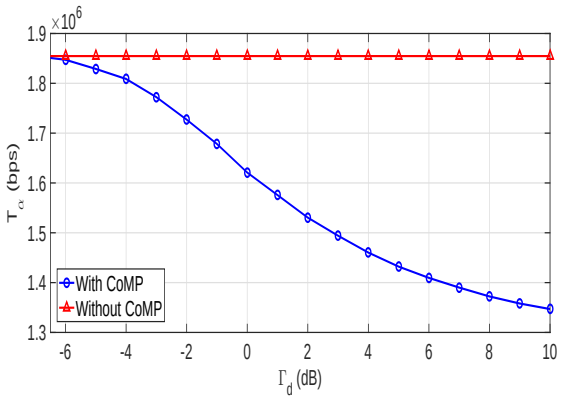

FIGURE 13: Variation of system throughput (T_α) with respect to CoMP SINR threshold (Γ_d), with and without CoMP, for $\mathcal{Z}_0$ pattern and PPP based BS distribution.

REFERENCES

[1] G. Fettweis and E. Zimmermann, "ICT energy consumption –trends and challenges," in *Proc. International Symposium on Wireless Personal Multimedia Communications (WPMC)*, 2008.

[2] J. T. Louhi, "Energy efficiency of modern cellular base stations," in *Proc. International Telecommunications Energy Conference (INTELEC)*, 2007.

[3] E. Oh, K. Son, and B. Krishnamachari, "Dynamic base station switching on/off strategies for green cellular networks," *IEEE Transactions on Wireless Communications*, vol. 12, no. 5, pp. 2126–2136, May 2013.

[4] A. Fehske, G. Fettweis, J. Malmodin, and G. Biczok, "The global footprint of mobile communications: the ecological and economic perspective," *IEEE Communications Magazine*, vol. 49, no. 8, pp. 55–62, 2011.

[5] N. Saxena, B. J. R. Sahu, and Y.S. Han, "Traffic-aware energy optimization in green LTE cellular systems," *IEEE Communications Letters*, vol. 18, no. 1, pp. 38–41, January. 2014.

[6] A. Kumar and C. Rosenberg, "Energy and throughput trade-offs in cellular networks using base station switching," *IEEE Transactions on Mobile Computing*, vol. 15, no. 2, pp. 364–376, February. 2016.

[7] S. S. Kumar and A. Kumar, "Energy efficient rate coverage with base station switching and load sharing in cellular networks,", in *Proc. International Conference on Communication Systems and Networks (COMSNETS)*, Bangalore, India, January 2016.

[8] J. Kim, W. S. Jeon, and D. G. Jeong, "Effect of base station-sleeping ratio on energy efficiency in densely deployed femtocell networks," in *IEEE Communications Letters*, vol. 19, no. 4, pp. 641–644, April 2015.

[9] C. Liu, B. Natarajan, and H. Xia, "Small cell base station sleep strategies for energy efficiency," *IEEE Transactions on Vehicular technology*, vol. 65, no. 3, pp. 1652–1661, March 2016.

[10] Y. L. Che, L. Duan, and R. Zhang, "Dynamic base station operation in large-scale green cellular networks," *IEEE Journal on Selected Areas in Communications*, vol. 34, no. 12, pp. 3127–3141, December 2016.

[11] 3GPP, "Overview of 3GPP Release 12," 3GPP RP 151570, V0.2.0, September, 2015.

[12] G. Nigam, P. Minero, and M. Haenggi, "Coordinated multipoint joint transmission in heterogeneous networks," *IEEE Transactions on Communications*, vol. 62, no. 11, pp. 4134–4146, November 2014.

[13] F. Baccelli and A. Giovanidis, "A stochastic geometry framework for analyzing pairwise-cooperative cellular networks," *IEEE Transactions on Wireless Communications*, vol. 14, no. 2, pp. 794–808, February 2015.

[14] X. Ge, H. Jin, J. Cheng, and V. C. M. Leung, "On fair resource sharing in downlink multi-point systems," *IEEE Communications Letters*, vol. 20, no. 6, pp. 1235–1238, June 2016.

[15] S. Y. Park, J. Choi, and D. J. Love, "Multicell cooperative scheduling for two-tier cellular networks," *IEEE Transactions on Communications*, vol. 62, no. 2, pp. 536–550, February 2014.

[16] C. L. I, C. Rowell, S. Han, Z. Xu, G. Li, and Z. Pan, "Toward green and soft: a 5G perspective," IEEE Communications Magazine, vol. 52, no. 2, pp. 66-73, February 2014.

[17] A. He, D. Liu, Y. Chen, and T. Zhangy, "Stochastic geometry analysis of energy efficiency in HetNets with combined CoMP and BS Sleeping," in *Proc. IEEE International Symposium on Personal, Indoor and Mobile Radio Communications (PIMRC)*, 2014, pp.1798–1802.

[18] F. Han, Z. Safar, and K. J. Ray Liu, "Energy efficient base station cooperative operation with guaranteed QoS," *IEEE Transactions on Communications*, vol. 61, no. 8, pp. 3505–3517, August 2013.

[19] S. Han, C. Yang, G. Wang, and M. Lei, "On the energy Efficiency of base station sleeping with multicell cooperative transmission," in *Proc. IEEE International Symposium on Personal, Indoor and Mobile Radio Communications (PIMRC)*, 2011, pp. 1536–1540.

[20] K. M. S. Huq, S. Mumtaz, J. Bachmatiuk, J. Rodriguez, X. Wang, and R. L. Aguiar, "Green HetNet CoMP: energy efficiency analysis and optimization," *IEEE Transactions on Vehicular Technology*, vol. 64,no. 10, pp. 4670–4683, October 2015.

[21] R. Yoghitha, and A. Kumar, "Base station switching with CoMP in cellular networks," in *Proc. National Conference on Communication (NCC)*, March 2016.

[22] P. H. Huang, S. S. Sun, and W. Liao, "GreenCoMP: Energy-Aware Cooperation for Green Cellular Networks," *IEEE Transactions on Mobile Computing*, vol. 16, no. 1, pp. 143–157, January 2017.

[23] S. Y. Kim and C. H. Cho, "Call Blocking Probability and Effective Throughput for Call Admission Control of CoMP Joint Transmission," *IEEE Transactions on Vehicular Technology*," vol. 66, no. 1, pp. 622–634, January 2017.

[24] S. Boyd and L. Vandenberghe, Convex Optimization. Cambridge, U.K.: *Cambridge Univ. Press*, 2004.

[25] 3GPP–TSG–RAN–WG1, "*Evolved universal terrestrial radio access (E-UTRA)*," 3GPP, Tech. Rep. TR 36.814, 2010.

[26] J. Wu, Y. Zhang, M. Zukerman, and E. K. N. Yung, "Energy-efficient base-stations sleep-mode techniques in green cellular networks: a survey," *IEEE Communication Surveys & Tutorials*, vol. 17, no. 2, second quarter 2015.

[27] D. Tse, P. Viswanath, Fundamentals of Wireless Communication. Cambridge, U.K.: *Cambridge Univ. Press*, 2006.

[28] D. Lopez-Perez, A. Ladanyi, A. Juttner, and J. Zhang, "Optimization method for the joint allocation of modulation schemes, coding rates, resource blocks and power in selforganizing LTE networks," in *Proc. IEEE International Conference on Computer Communications (INFOCOM)*, Shanghai, China, April 2011, pp. 111–115.

[29] J. Ghimire and C. Rosenberg, "Revisiting scheduling in heterogenous networks when the backhaul is limited," *IEEE Journal on Selected Areas in Communications*, vol. 33, no. 10, October 2015.